# Acetylenyl-Linked, Porphyrin-Bridged, Donor−Acceptor Molecules: A Theoretical Analysis of the Molecular First Hyperpolarizability in Highly Conjugated Push−Pull Chromophore Structures

**Satyam Priyadarshy,[‡] Michael J. Therien,[†] and David N. Beratan*[,‡]**

*Contribution from the Department of Chemistry, University of Pittsburgh, Pittsburgh, Pennsylvania 15260, and Department of Chemistry, University of Pennsylvania, Philadelphia, Pennsylvania 19104-6323*

*Received August 8, 1995*[⊗]

**Abstract:** We describe the theoretical basis for the exceptionally large molecular first hyperpolarizabilities inherent to (5,15-diethynylporphinato)metal-bridged donor−acceptor (D−A) molecules. $\beta$ values relevant for hyper-Rayleigh experiments are calculated at 1.064 and 0.830 $\mu$m for a complex with such a structure, [5-((4′-(dimethylamino)-phenyl)ethynyl)-15-((4″-nitrophenyl)ethynyl)-10,20-diphenylporphinato]zinc(II), and are 472 × $10^{-30}$ and 8152 × $10^{-30}$ $cm^5$/esu, respectively. The values are 1 order of magnitude larger than that calculated for any other porphyrin bridged donor−acceptor chromophore studied to date. The considerably enhanced hyperpolarizability arises from the significant excited-state electronic asymmetry manifest in such structures (derived from the strong bridge-mediated D−A coupling enabled by the largely porphyrin-based excited state) and the large bridge-centered oscillator strength in this new class of D−bridge−A molecules. Our analysis of NLO properties (based upon INDO/SCI calculations within the sum over states formalism) shows a sensitivity to the degree of cumulenic character in the ground state. Calculations on structurally related *multi*porphyrin systems suggest candidate chromophores with further enhanced optical nonlinearities.

## 1. Introduction

The continued interest in molecules that possess large quadratic nonlinear optical (NLO) properties has motivated considerable interplay between molecular synthesis and theory.[1−9] The general approach to designing NLO chromophores with large molecular first-order hyperpolarizabilities ($\beta$ values), that might be appropriate for the eventual development of processable optoelectronic materials and devices, has involved coupling both an electron donor (D) and acceptor (A) to an organic framework that provides moderately strong electronic coupling between D and A. While a finite amount of D−A coupling is essential for a significant first hyperpolarizability, the coupling mediated by the organic scaffolding must not be so strong as to remove the electronic asymmetry provided by the donor and acceptor groups.

It has been recognized that macrocycles with extensive $\pi$-conjugation may provide a basis from which to elaborate D−A molecules with interesting NLO properties.[10,11] For example, early theoretical work by Ratner and Marks predicted that electronically asymmetric phthalocyanines should have good, but not unusually large, molecular first-order hyperpolarizabilities ($\beta \sim 165 \times 10^{-30}$ $cm^5$/esu at 1.907 $\mu$m).[11] Experimentally, Suslick has examined a series of porphyrin molecules *meso*-substituted with both 4′-(dimethylamino)phenyl and 4″-nitrophenyl moieties. These electronically asymmetric or "push−pull" porphyrins were shown to possess modest molecular first-order hyperpolarizabilities on the order of 30 × $10^{-30}$ $cm^5$/esu.[10] These experimental $\beta$ values were obtained from electric-field-induced second-harmonic generation (EFISH) experiments in which the incident irradiation was 1.91 $\mu$m, with the magnitude of the molecular first hyperpolarizability corresponding to the projection of the vector component of the $\beta$ tensor onto the molecular dipole.

Recently, the unusually large molecular first-order hyperpolarizabilities of a new class of electronically asymmetric porphyrin molecules were reported.[12] These systems are based on a porphyrin-centered 5,15-bis(arylethynyl) linkage topology[13,14] and constitute a new class of highly conjugated chromophores that feature an ethynyl unit bridging the carbon

[‡] University of Pittsburgh.
[†] University of Pennsylvania.
[⊗] Abstract published in *Advance ACS Abstracts,* December 1, 1995.

(1) Beratan, D. N. In *Materials for Nonlinear Optics: Chemical Perspectives*; ACS Symposium Series; Marder, S. R., Sohn, J. E., Stucky, G. D., Eds.; American Chemical Society: Washington, DC, 1991; Vol. 455, pp 89−102.
(2) Boyd, R. W. *Nonlinear Optics*; Academic Press: New York, 1992.
(3) Brédas, J. L.; Silbey, R. J. *Conjugated Polymers. The Novel Science and Technology of Highly Conducting and Nonlinear Optically Active Materials*; Kluwer: Dordrecht: The Netherlands, 1991.
(4) Burland, D. M. *Chem. Rev.* **1994**, *94*, 1.
(5) *Nonlinear Optical Properties of Organic Molecules and Crystals*; Chemla, D. S.; Zyss, J., Eds.; Academic Press: New York, 1987; Vols. 1 and 2.
(6) Denning, R. G. In *Spectroscopy of New Materials*; Clarke, R. J. H., Hester, R. E., Eds.; John Wiley & Sons, Ltd: London, 1993.
(7) *Nonlinear Optical Properties of Polymers*; Heeger, A. J., Orenstein, J., Ulrich, D. R., Eds.; Materials Research Society Symposium Proc. 109, MRS, Pittsburgh, PA, 1988.
(8) Khananrian, G., Ed. *Nonlinear Optical Properties of Organic Molecules III. Proc. SPIE−Int. Soc. Opt. Eng.* 1990, pp 1337.
(9) *Materials for Nonlinear Optics: Chemical Perspectives*; Marder, S. R., Sohn, J. E., Stucky, G. D., Eds.; American Chemical Society: Washington, DC, 1991; Vol. 455.
(10) Suslick, K. S.; Chen, C. T.; Meredith, G. R.; Cheng, L.-T. *J. Am. Chem. Soc.* **1992**, *114*, 6928−6930.
(11) Li, D. Q.; Ratner, M. A.; Marks, T. J. *J. Am. Chem. Soc.* **1988**, *110*, 1707−1715.
(12) LeCours, S. M.; Guan, H.-W.; DiMagno, S. G.; Wang, C. H.; Therien, M. J. *J. Am. Chem. Soc.* **1996**, *118*, 1497−1503.
(13) LeCours, S. M.; DiMagno, S. G.; Therien, M. J. *J. Am. Chem. Soc.*, submitted.

0002-7863/96/1518-1504$12.00/0 

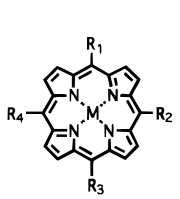


Ph = 

a = 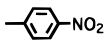


d = 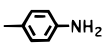


D = 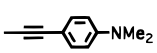


A = 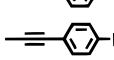


| $R_1$ | $R_3$ | $R_2$ | $R_4$ | M | Compound | |
|---|---|---|---|---|---|---|
| Ph | Ph | H | H | Zn | ZnDPP | (I) |
| Ph | Ph | D | H | Zn | D-ZnDPP | (II) |
| Ph | Ph | H | A | Zn | ZnDPP-A | (III) |
| Ph | Ph | D | A | Zn | D-ZnDPP-A | (IV) |
| Ph | Ph | d | a | $H_2$ | d-$H_2$DPP-a | (V) |
| d | a | d | a | $H_2$ | $d_2$-$H_2$P-$a_2$ | (VI) |
| d | d | d | a | $H_2$ | $d_3$-$H_2$P-a | (VII) |
| d | a | a | a | $H_2$ | d-$H_2$P-$a_3$ | (VIII) |

**Figure 1.** Porphyrin, donor−porphyrin, porphyrin−acceptor, and donor−porphyrin−acceptor molecules considered in this computational study.

frameworks of adjacent aromatic systems.[15] Hyper-Rayleigh (light) scattering studies show that one such chromophore featuring the push−pull arylethynyl structural motif, [5-((4′-(dimethylamino)phenyl)ethynyl)-15-((4″-nitrophenyl)ethynyl)-10,20-diphenylporphinato]zinc(II), (D−ZnDPP−A) (see Figure 1) possesses by far the largest $\beta$ value yet measured ($4933 \times 10^{-30}$ cm$^5$/esu at 1.064 $\mu$m) for an organic-based chromophore. The photophysical properties of this molecule and related structures are unusual in that they evince considerable charge transfer character mixed into the porphyrin B- and Q-type transitions.[12,14,16]

In this paper, we present a theoretical study of the electronic structure and NLO properties of D−ZnDPP−A and its constituent molecular components using the sum over states approach in which the electronic states are calculated via the semiempirical INDO/SCI method. We compare these results with those obtained from a standard two-state analysis and contrast them with those calculated for related compounds.

## 2. Methodology

The linear and nonlinear optical properties of the D−porphyrin−A molecule featuring the arylethynyl structural topology along with several related structures are investigated here at the semiempirical level. The calculated frequency-dependent molecular first-order hyperpolarizability for these molecular systems is based on the sum over states (SOS) approach.[17] The states are calculated with the semiempirical INDO/SCI method (intermediate neglect of differential overlap/singly excited configuration interaction). A detailed discussion of the INDO/SCI-SOS technique was given recently by Ratner and Kanis.[18−20] In this approach, the Cartesian components of the $\beta$ tensor are given by

$$\beta_{ijk} = \beta_{ijk,2} + \beta_{ijk,3} \tag{1}$$

Here, the subscripts 2 and 3 refer to two-level and three-level contributions to the SOS expression for $\beta$. These terms derive their names from the number of states, including the ground state, that enter the $\beta$ expression (eqs 2 and 3). The summations in these equations are

$$\beta_{ijk,2} = -\frac{e^3}{2\hbar^2}\sum_{m\neq g}[r^j_{gm}r^k_{gm}\Delta r^i_m(\omega^2_{mg} - 4\omega^2) + r^i_{gm}(r^k_{gm}\Delta r^j_m + r^j_{gm}\Delta r^k_m(\omega^2_{mg} + 2\omega^2)]\frac{1}{(\omega^2_{mg} - \omega^2)(\omega^2_{mg} - 4\omega^2)} \tag{2}$$

$$\beta_{ijk,3} = -\frac{e^3}{8\hbar^2}\sum_{n\neq g}\sum_{\substack{m\neq g\\ m\neq n}}\Bigg[(r^j_{gn}r^i_{nm}r^k_{gm} + r^k_{gn}r^i_{nm}r^j_{gm})\left\{\frac{1}{(\omega_{ng} - \omega)(\omega_{mg} + \omega)} + \frac{1}{(\omega_{ng} + \omega)(\omega_{mg} - \omega)}\right\} + (r^i_{gn}r^j_{nm}r^k_{gm} + r^i_{gn}r^k_{nm}r^j_{gm})\left\{\frac{1}{(\omega_{ng} + 2\omega)(\omega_{mg} + \omega)} + \frac{1}{(\omega_{ng} - 2\omega)(\omega_{mg} - \omega)}\right\} + (r^j_{gn}r^k_{nm}r^i_{gm} + r^k_{gn}r^j_{nm}r^i_{gm})\left\{\frac{1}{(\omega_{ng} - 2\omega)(\omega_{mg} - \omega)} + \frac{1}{(\omega_{ng} + \omega)(\omega_{mg} + 2\omega)}\right\}\Bigg] \tag{3}$$

carried out over the electronic excited states. In eqs 2 and 3, $\omega$ is the frequency of the applied electric field, $r^s_{nm}$ ($\langle n|r^s|m\rangle$) is the matrix element of the position operator $r^s$ (along the sth coordinate axis) between the electronic states $|n\rangle$ and $|m\rangle$. The energy separation between the ground state $|g\rangle$ and an excited state $|n\rangle$ is $\hbar\omega_{ng}$ while the dipole moment difference between these states is $\Delta r^s_n = (r^s_{nn} - r^s_{gg})$.

The INDO/SCI-SOS formalism allows the computation of all 27 tensor components of $\beta$. A useful comparison with the results of the EFISH (electric-field-induced second-harmonic generation) experiment requires the projection of the $\beta$ vector onto the dipole moment vector, $\mu$:

$$\beta_{\text{vec}} = \frac{\beta\mu}{|\mu|} = \frac{\sum_s \beta_s\mu_s}{\sqrt{\sum_s \mu_s^2}} \tag{4}$$

Here, $s$ spans the three Cartesian axes. The $\beta$ component along the $s$ axis ($\beta_s$) is given by

$$\beta_s = \beta_{sss} + \frac{1}{3}\sum_{\alpha\neq s}(\beta_{s\alpha\alpha} + 2\beta_{\alpha\alpha s}) \tag{5}$$

In eqs 4 and 5, the $\beta$ tensor elements of eq 1 are used to evaluate $\beta_{\text{vec}}$, where $\alpha = x, y$, and $z$. Expressions for $\beta_{\text{vec},2}$ and $\beta_{\text{vec},3}$, the vector projections of $\beta$ derived from the two- and three-level terms, are also computed using eqs 4 and 5, respectively. Further reference to $\beta$ in the paper refers to $\beta_{\text{vec}}$.

Comparing the magnitudes of the molecular first-order hyperpolarizabilities obtained from hyper-Rayleigh scattering (HRS) studies[21] does not require the computation of $\beta$ projected onto $\mu$ (eq 4), since the orientation averaged value ($\beta_s$) is the relevant parameter and is evaluated directly. In the HRS experiment, there exists a relation between the microscopic hyperpolarizability in laboratory coordinates ($\beta_{ZZZ}$) and that in the molecular reference frame ($\beta_{zzz}$); a detailed discussion of this

(14) LeCours, S. M.; de Paula, J. C.; Therien, M. J. *J. Phys. Chem.*, submitted.
(15) Lin, V. S.-Y.; DiMagno, S. G.; Therien, M. J. *Science (Washington, DC)* **1994**, *264*, 1105−1111.
(16) LeCours, S. M.; Williams, S. A.; Therien, M. J. Manuscript in preparation.
(17) Ward, J. F. *Rev. Mod. Phys.* **1971**, *37*, 1−18.
(18) Kanis, D. R.; Ratner, M. A.; Marks, T. J. *Chem. Rev.* **1994**, *94*, 195−242.
(19) Kanis, D. R.; Marks, T. J.; Ratner, M. A. *Nonlinear Optics* **1994**, *6*, 317−335.
(20) Kanis, D. R.; Lacroix, P. G.; Ratner, M. A.; Marks, T. J. *J. Am. Chem. Soc.* **1994**, *116*, 10089−10102.

has been presented by Hendrickx.[22] This relation is given as

$$\langle\beta^2_{ZZZ}\rangle = \frac{1}{7}\sum_s \beta^2_{sss} + \frac{6}{35}\sum_{\alpha\neq s}\beta_{sss}\beta_{s\alpha\alpha} + \frac{9}{35}\sum_{\alpha\neq s}\beta^2_{ss\alpha} + \frac{6}{35}\sum_{s,t,u,\mathrm{cyc}}\beta_{sst}\beta_{tuu} + \frac{12}{35}\beta^2_{stu} \quad (6)$$

Here, cyc means cyclic permutation of coordinate indexes. In HRS expressions, an isotropic average is made for all the molecular $\beta$ tensor components, indicating that the HRS is sensitive to all such elements. For dipolar molecules, where the molecular tensor component in the direction of the charge transfer axis is the largest, the values of ($\beta_{ZZZ}$) and ($\beta_{zzz}$) are expected to be the same.

The SOS calculation of $\beta$ appears to reach a limiting value as the number of the excited states included in the summations of eqs 4 and 5 increases beyond ~10 excited states. A summation over 25−400 excited states has been shown to be adequate for reliable $\beta$ estimates in many cases.[12,23] In this study, we calculate $\beta$ by summing over 51 excited states. Configuration interaction (CI) was applied to 1500 singly excited configurations to obtain excited-state properties, after a closed-shell self-consistent Hartree−Fock calculation at the INDO level (intermediate neglect of differential overlap).[24]

Molecular geometries for compounds **II**−**IV** (Figure 1), which possess either one or two *meso*-arylethynyl groups, were optimized using the AM1 method as parameterized within the MOPAC93.0[25] program. The dihedral angle between the *meso*-phenyl groups and the porphyrin ring system was calculated to be 62.3°, in good agreement with the experimental data.[26−28] For the case of the *meso*-(arylethynyl)-phenyl rings, no steric barrier prevents these groups from attaining a coplanar relationship with respect to the porphyrin plane. Maximum $\pi$ overlap is attained for an all planar configuration of the three aromatic ring systems that are bisected by the mirror plane that defines the $C_s$ point group for the D−ZnDPP−A (IV) complex; our calculations predict that this is the lowest energy conformation. For the sake of computational simplicity, only this molecular geometry for the arylethynyl moieties was considered in our electronic structure and NLO calculations on compounds **II**−**IV**. The (5,10-diphenylporphinato)-zinc geometry (ZnDPP, **I**) was also optimized at the AM1 level. For these theoretical studies, the aryl rings in 5-(4′-aminophenyl)-15-(4″-nitrophenyl)-10,20-diphenylporphyrin (d−$H_2$DPP−a, **V**), 5,10-bis(4′-aminophenyl)-15,20-bis(4″-nitrophenyl)porphyrin (d$_2$−$H_2$P−a$_2$, **VI**), 5,10,15-tris(4′-aminophenyl)-20-(4″-nitrophenyl)porphyrin (d$_3$−$H_2$P−a, **VII**), and 5-(4′-aminophenyl)-10,15,20-tris(4″-nitrophenyl)porphyrin (d−$H_2$P−a$_3$, **VIII**) were assumed to adopt an optimal dihedral angle similar to that calculated for the unsubstituted phenyl rings of ZnDPP. The details of geometry optimization of these molecules are presented elsewhere.[29] These structures are shown in Figure 1.

## 3. Results and Discussion

**Ground- and Excited-State Properties.** Figure 2 shows the energies of the frontier occupied and unoccupied molecular orbitals for structures **I**−**IV**. A more detailed investigation of the molecular orbitals of **I** is presented elsewhere.[29] Since we assume $C_{2h}$ symmetry for ZnDPP, the LUMO of this (porphinato)zinc complex is nondegenerate.

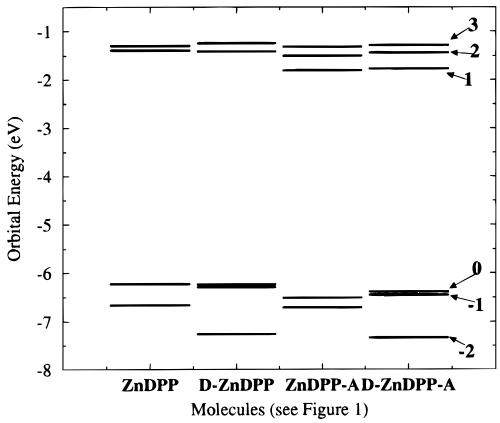


**Figure 2.** Energies of the frontier orbitals of D−ZnDPP−A molecules and its fragments.

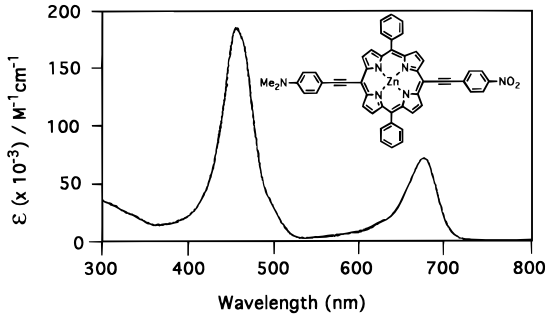


**Figure 3.** Electronic spectrum of 5-((4′-(dimethylamino)phenyl)-ethynyl)-15-((4″-nitrophenyl)ethynyl)-10,20-diphenylporphinato]zinc-(II) (D−ZnDPP−A, **IV**) recorded in chloroform.

In [5-((4′-(dimethylamino)phenyl)ethynyl)-10,20-diphenylporphinato]zinc(II) (D−ZnDPP, **II**), mixing of the highest occupied orbitals of the ZnDPP bridge with the D ((4′-(dimethylamino)-phenyl)ethynyl) fragment leads to a nearly degenerate HOMO. The nearly degenerate HOMO has the same energy as the HOMO of ZnDPP, while the HOMO−2 lies 0.9 eV below the nearly degenerate HOMO. These molecular orbitals have a significant contribution from the arylethynyl phenyl ring $\pi$-electrons. In the case of [5-((4′-nitrophenyl)ethynyl)-10,20-diphenylporphinato]zinc(II) (ZnDPP−A, **III**), the acceptor orbitals lower the LUMO energy relative to ZnDPP. The near degeneracy of the HOMO in D−ZnDPP is lifted when the A ((4″-nitrophenyl)ethynyl) fragment replaces the H atom at the porphyrin 15-position of D−ZnDPP. It is also worthy of note that the LUMO+1 and LUMO+2 of both ZnDPP−A and D−ZnDPP−A become degenerate due largely to the strong mixing of the porphyrin-based $\pi$-orbital with those of the A fragment. Thus, in D−ZnDPP−A, the frontier orbitals have significant contributions from the phenyl and acetylenyl $\pi$-orbitals of the D and A arylethynyl fragments.

Figure 3 shows the experimental absorption spectrum of D−ZnDPP−A. D−ZnDPP−A, and other 5,15-bis(arylethynyl)-porphyrins exhibit dramatic red shifts in the porphyrin B- and Q-type transitions that are unparalleled for porphyrins featuring a nondistorted, planar ring structure.[13,14] The experimental B- and Q-type transitions of D−ZnDPP−A lie 2574 and 2491 cm$^{-1}$ to the red, respectively, of the B(0,0) and Q(0,0) bands of ZnDPP. The broadening of these transitions in D−ZnDPP−A relative to ZnDPP is equally striking: for example, the full width at half-maximum (FWHM) of the B band of ZnDPP is 719 cm$^{-1}$ while that of D−ZnDPP−A is 2050 cm$^{-1}$. Moreover, the

(21) (a) Terhune, R. W.; Maker, P. D.; Savage, C. M. *Phys. Rev. Lett.* **1965**, *14*, 681−684. (b) Clays, K.; Persoons, A. *Phys. Rev. Lett.* **1991**, *66*, 2980−2983. (c) Clays, K.; Hendrickx, E.; Triest, M.; Persoons, A.; Dehu, C.; Bredas, J. L. *Science (Washington, DC)* **1993**, *262*, 1419−1421. (d) Laidlaw, M.; Denning, R. G.; Verbiest, T.; Chauchard, E.; Persoons, A. *Nature (London)* **1993**, *363*, 58−60. (e) Pauley, M. A.; Wang, C. H.; Jen, A. K.-Y. *J. Chem. Phys.* **1995**, *102*, 6400−6405.

(22) Hendrickx, E.; Clays, K.; Persoons, A.; Dehu, C.; Bredas, J. L. *J. Am. Chem. Soc.* **1995**, *117*, 3547−3555.

(23) Kanis, D. R.; Ratner, M. A.; Marks, T. J. *J. Am. Chem. Soc.* **1992**, *114*, 10338−10357.

(24) (a) Ridley, J.; Zerner, M. C. *Theor. Chim. Acta (Berlin)* **1973**, *32*, 111−134. (b) Parkinson, W. A.; Zerner, M. C. *J. Chem. Phys.* **1989**, *90*, 5606−5611.

(25) (a) Dewar, M. J. S.; Zoebisch, E. G.; Healy, E. F.; Stewart, J. J. P. *J. Am. Chem. Soc.* **1985**, *107*, 3902−3909. (b) Stewart, J. J. P. *Mopac 93.0 Manual*; Fujitsu Limited; Tokyo, 1993.

(26) Eriksson, S.; Källebring, B.; Larsson, S.; Martensson, J.; Wennerström, O. *Chem. Phys.* **1990**, *146*, 165−177.

(27) Scheidt, W. R.; Kastner, M. E.; Hatano, K. *Inorg. Chem.* **1978**, *17*, 706.

(28) Prendergast, K.; Spiro, T. G. *J. Phys. Chem.* **1991**, *95*, 9728−9736.

(29) Priyadarshy, S.; Beratan, D. N. Manuscript in preparation.

**Table 1.** Q and Soret Band Transition Properties for Compounds **I**−**VIII**[a]

| | ZnDPP | D−ZnDPP−A | D−ZnDPP | ZnDPP−A | d−$H_2$DPP−a | $d_2$−$H_2$P−$a_2$ | $d_3$−$H_2$P−a | d−$H_2$P−$a_3$ |
|---|---|---|---|---|---|---|---|---|
| $Q_x$ | 16.0 (0.030) [18.5] | 15.3 (0.144) [14.8] | 15.9 (0.012) | 15.8 (0.028) | 14.4 (0.002) | 14.4 (0.001) | 14.4 (0.002) | 14.4 (0.002) |
| $Q_y$ | 16.0 (0.050) | 15.4 (0.016) | 15.9 (0.011) | 15.8 (0.014) | 16.7 (0.001) | 16.6 (0.001) | 16.6 (0.001) | 16.6 (0.001) |
| $B_x$ | 28.4 (3.760) [24.3] | 24.1 (3.462) [21.7] | 25.9 (3.181) | 24.8 (2.635) | 26.2 (0.824) | 26.3 (1.275) | 26.6 (2.204) | 25.6 (0.607) |
| $B_y$ | 29.1 (2.849) | 26.8 (1.582) | 27.8 (3.037) | 26.8 (0.799) | 27.1 (1.182) | 26.3 (1.547) | 27.1 (2.579) | 26.8 (0.842) |
| | | 26.6 (0.565) | 30.3 (0.102) | 28.8 (2.632) | 27.7 (0.742) | 27.6 (0.228) | 28.1 (0.097) | 27.5 (1.225) |
| | | 28.3 (1.461) | | | 28.3 (2.536) | 27.9 (0.109) | 28.5 (0.032) | 28.0 (2.680) |

[a] The transition energies are given in units of $10^{+3}$ $cm^{-1}$. The theoretical oscillator strengths are displayed in parentheses. The experimental values of the transition energies are given in square brackets (see also ref 12).

**Table 2.** Composition of the Excited-State Wave Functions of ZnDPP and D−ZnDPP−A in Terms of the Linear Combination Coefficients in the Configuration Expansion (only coefficients larger than 0.1 are reported)[a]

| | ZnDPP |
|---|---|
| $Q_x$ | $0.65\ \Psi_{-1\rightarrow1} - 0.72\ \Psi_{0\rightarrow2}$ |
| $Q_y$ | $0.63\ \Psi_{-1\rightarrow2} + 0.77\ \Psi_{0\rightarrow1}$ |
| $B_x$ | $-0.12\ \Psi_{-10\rightarrow2} - 0.74\ \Psi_{-1\rightarrow2} + 0.62\ \Psi_{0\rightarrow1}$ |
| $B_y$ | $-0.14\ \Psi_{-10\rightarrow1} - 0.73\ \Psi_{-1\rightarrow1} - 0.65\ \Psi_{0\rightarrow2}$ |
| | **D−ZnDPP−A** |
| $Q_x$ | $0.12\ \Psi_{-2\rightarrow1} - 0.63\ \Psi_{-1\rightarrow2} + 0.66\ \Psi_{0\rightarrow1} + 0.34\ \Psi_{0\rightarrow3}$ |
| $Q_y$ | $-.013\ \Psi_{-2\rightarrow2} - 0.66\ \Psi_{-1\rightarrow1} - 0.36\ \Psi_{-1\rightarrow3} - .64\ \Psi_{0\rightarrow2}$ |
| $B_x$ | $-0.18\ \Psi_{-3\rightarrow1} + 0.17\ \Psi_{-3\rightarrow3} + 0.22\ \Psi_{-2\rightarrow2} + 0.12\ \Psi_{-2\rightarrow4} - 0.55\ \Psi_{-1\rightarrow2} - 0.66\ \Psi_{0\rightarrow1} + 0.27\ \Psi_{0\rightarrow2} + 0.12\ \Psi_{0\rightarrow5}$ |
| $B_y$ | $-0.18\ \Psi_{-3\rightarrow1} + 0.17\ \Psi_{-3\rightarrow3} + 0.22\ \Psi_{-2\rightarrow2} + 0.12\ \Psi_{-2\rightarrow4} - 0.55\ \Psi_{-1\rightarrow2} - 0.66\ \Psi_{0\rightarrow1} + 0.27\ \Psi_{0\rightarrow2} + 0.12\ \Psi_{0\rightarrow5}$ |

[a] Here, subscripts correspond to the following orbitals: The highest occupied orbitals have index 0, i.e. 0 = HOMO, while all other occupied orbitals have index −1, −2, ..., −*n*, which correspond to HOMO−1, HOMO−2, ..., HOMO−*n*, respectively. LUMO = 1, LUMO+1 = 2, LUMO+2 = 3, and so on; therefore, *n* = LUMO + *n*−1 orbital. (See Figure 2).

electronic spectra of the 5,15-bis(arylethynyl)porphyrins evince considerable augmentation of the B- and Q-band oscillator strengths, with the relative enhancement of the Q band being particularly impressive.[12−14]

These features are consistent with the calculated electronic structure and can be understood from Table 1, which lists the calculated transition energies for the porphyrin-based NLO chromophores considered in this study. While the absolute magnitudes of the transition energies do not correlate with the experimental electronic spectra of these compounds, INDO/SCI calculations are known to predict spectral transitions within 2000 $cm^{-1}$ of experimental transition energies; moreover, these calculations mirror well the experimental energy gap between the porphyrin B- and Q-transitions and do exceptionally well in modeling the relative oscillator strengths of the major bands in the electronic spectrum. Our calculations show the $Q_x$ and $Q_y$ transitions in ZnDPP to be approximately degenerate with weak oscillator strength, in contrast to that observed for D−ZnDPP−A. There is a small splitting of ∼100 $cm^{-1}$ between the $Q_x$ and $Q_y$ transitions of D−ZnDPP−A. Consistent with a variety of photophysical studies that show 5,15-bis-(arylethynyl)porphyrins to possess a highly polarized excited state,[12−16] we calculate the oscillator strength of the D−ZnDPP−A $Q_x$ transition to be 0.14, 10 times stronger than that of the $Q_y$ transition; moreover, the $Q_x$ transition is approximately 100 times stronger than that of any other porphyrin considered in this study (Table 1). These calculations thus reproduce the salient features of the experimental D−ZnDPP−A absorption spectrum. The calculated $B_x$ and $B_y$ transitions of ZnDPP occur at 352 and 343 nm, respectively. In the case of D−ZnDPP−A, the calculations predict two strong Soret transitions ($B_x$ at 405 nm and $B_y$ at 372 nm). These absorptions are red shifted relative to the ZnDPP B band, in agreement with experiment. A few other very weak transitions within the 350−415 nm range are also calculated.

In Table 1, the calculated Q and Soret transitions for the push−pull free base porphyrins synthesized and studied by Suslick[10] (**VI**−**VIII**) are reported, along with a compound structurally related to D−ZnDPP−A and the Suslick push−pull porphyrins, d−$H_2$DPP−a (**V**). Theory predicts that all of these electronically asymmetric porphyrins have very weak Q-band transitions, although the bands themselves are red shifted compared to those of both ZnDPP and D−ZnDPP−A. The calculated oscillator strengths of the Soret transitions in **V**−**VIII** are not as strong for the B-band transition in D−ZnDPP−A, a fact borne out by the collected experimental data for these systems.

In Table 2, the excited-state wave functions are compared. The compositions of the Q and B transitions of ZnDPP follow those predicted by Gouterman's four-orbital model.[30] In this model, the four excited states ($Q_x$, $Q_y$, $B_x$, and $B_y$) are obtained as linear combinations of the singly excited configurations generated by promoting an electron from the two highest occupied to the two lowest unoccupied molecular orbitals of the porphyrin chromophore. In the case of D−ZnDPP−A, the four-orbital model may not be strictly applicable to the electronic spectral analysis, since our calculations show that there is a significant contribution from excited configurations that involve molecular orbitals lying below HOMO−1 and above LUMO+1.[29,30]

**Nonlinear Optical Properties.** Figure 4 shows $\beta$ as a function of the number of excited basis states (EBS) included in the calculation (eq 1) for molecules **II**−**IV**. The $\beta$ values apparently converge as the number of excited states increases beyond 20. $\beta$ increases initially and then decreases as the number of EBS in the summation is increased. This same behavior is seen in numerous smaller chromophores, such as *p*-nitroaniline, para-substituted oligophenylene compounds, and electronically asymmetric diphenylacetylenes.[31] $\beta$ is shown in Figure 4 for four specific incident wavelengths; the 1.064 and 0.830 $\mu$m values of $\lambda_{input}$ coincide with experimental incident irradiation wavelengths used to determine the molecular first hyperpolarizability for D−ZnDPP−A.[12] INDO/S calculations for porphyrins are known to predict Soret transitions at wavelengths shorter than the experimental values [$\lambda_{max}$(experiment) = 460 nm and $\lambda$(calculated)) = 405 nm]. As a simple attempt to compensate for this systematic offset between the computed and observed Soret transition wavelengths, we also report $\beta$ at 0.92 $\mu$m (offset from 1.064 $\mu$m) and 0.74 $\mu$m (offset from 0.830 $\mu$m), which are wavelength shifted by the difference

(30) Gouterman, M. J. *J. Mol. Spectrosc.* **1961**, *6*, 138.
(31) Dehu, C.; Brédas, J. L. *Int. J. Quantum Chem.* **1994**, *52*, 89−96.

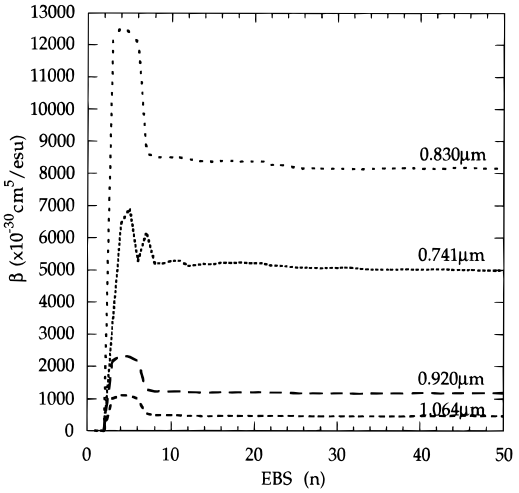


**Figure 4.** $\beta_{vec}$ (see eq 4) plotted as a function of excited basis states (EBS). Values at 1.064 and 0.830 $\mu$m coincide with experimental wavelengths.[12] As a simple attempt to correct for the fact that INDO/S calculated and experimental measures of the Soret wavelength do not match perfectly, we also computed $\beta$ at wavelengths offset (0.92 and 0.74 $\mu$m, see text) from the computed Soret transition by an amount equal to the offset between the experimental incident wavelength and the experimental Soret transition wavelength. Calculated values of $\beta_{zzz}$ at 740 nm are negative, but in an HRS experiment, one measures the absolute values (see eq 6), so the absolute values are plotted here.

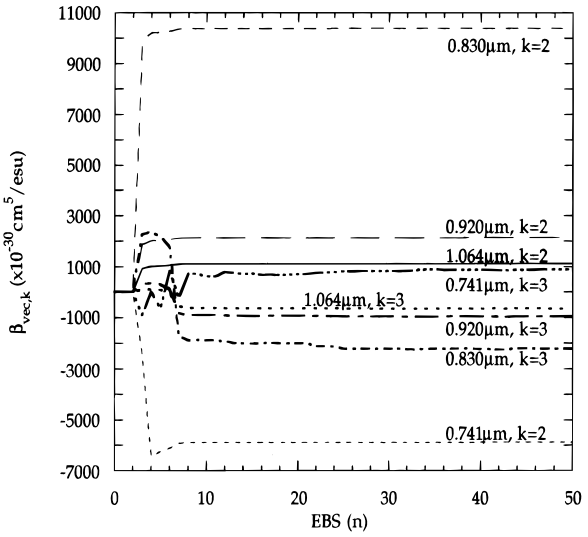


**Figure 5.** $\beta_{vec,k}$ components plotted as a function of excited basis states (EBS).

in the computed and observed Soret transition wavelength. As such, comparison of the computed $\beta$ values at these offset wavelengths with the experimental values may be appropriate.

Figure 5 shows two-level ($\beta_{vec,2}$) and three-level ($\beta_{vec,3}$) contributions to $\beta_{vec}$ versus the number of excited states in the sum of eq 1.[20] The contributions from $\beta_{vec,2}$ and $\beta_{vec,3}$ are of opposite sign. As the number of excited states increases beyond 20, the two contributions apparently reach limiting values.

Figure 6, shows a charge distribution diagram for the first 10 EBS's. The qualitative differences in charge distribution between the ground and excited states in D−ZnDPP−A are easily seen in this plot. For simplicity, the electronic charge distribution is put into bins corresponding to the net positive or negative charge localized on the D, ZnDPP, or A fragments of the D−ZnDPP−A chromophore (see Figure 1). The key EBS's that influence $\beta$ are apparent. For example, the state $S_3$ contributes significantly to $\beta$ as it is the first charge transfer state with a buildup of electron density on A and a decrease in electron density on both D and ZnDPP. State $S_4$ reduces $\beta$

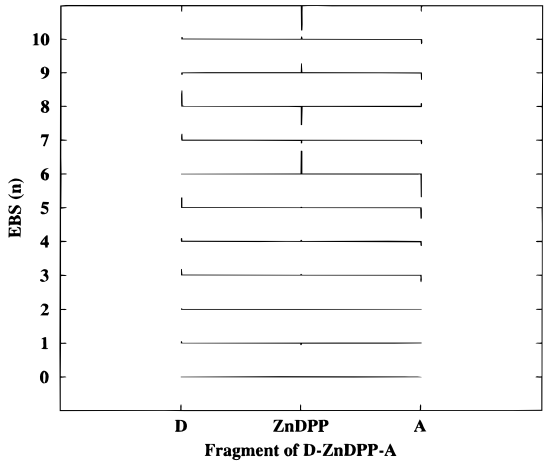


**Figure 6.** Localized excited-state charge on the donor, bridge, and acceptor portions of D−ZnDPP−A. The direction and magnitude of the vertical lines correspond to the sign and relative charge density on the D, ZnDPP, or A fragments in a given excited state.

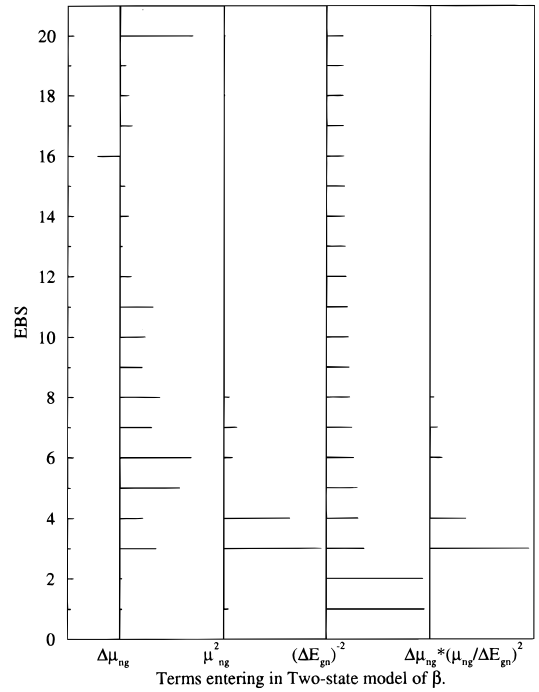


**Figure 7.** Terms entering the two-state model of $\beta$. Note that these terms arise from the INDO/S calculation are frequency independent.

slightly, perhaps as a consequence of a small increase of electron density on ZnDPP and on D. A general observation is that, when there is a buildup of electron density on the bridge (ZnDPP), $\beta$ is reduced by the addition of this contribution to the previous value. There are some exceptions to this simple rule, which are resolved if one looks at other related properties of a particular state. These properties, shown in Figure 7, are dipole moment compared to the ground state ($\Delta\mu_{ng}$), the square of the transition dipole moment ($\mu^2_{ng}$), and the inverse square of the excited-state energy ($\Delta E_{gn}{}^{-2}$) with respect to the ground state. The product of the prior three terms ($\Delta\mu_{ng}\mu^2_{ng}\Delta E_{gn}{}^{-2}$) enters the simple two-state approximation for $\beta$. The dependence of $\beta$ in the sum over EBS clearly reflects the sizes of the $\Delta\mu_{ng}$, $\mu^2_{ng}$, and $\Delta E_{gn}{}^{-2}$ terms. A comparison of Figures 4 and 7 clearly shows that the dependence of $\beta$ is reflected by the $\Delta\mu_{ng}\mu^2_{ng}\Delta E_{gn}{}^{-2}$ product for molecules **II**−**IV**. Quantitating the degree of charge transfer and the two-state contributions to the EBS provides an understanding of the origin of $\beta$ in these structures. Beyond 20 excited states, there is no significant

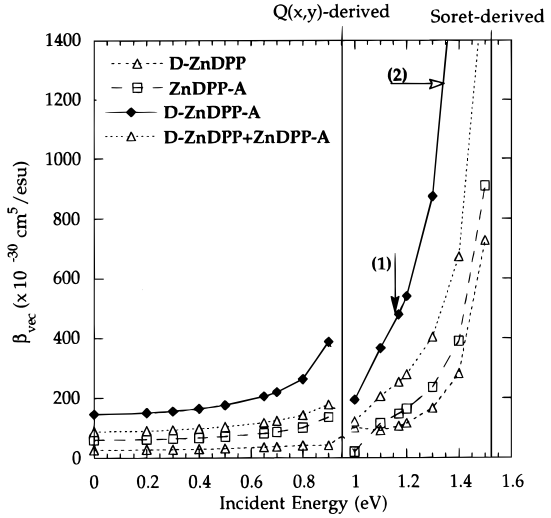


**Figure 8.** $\beta_{vec}$ (see eq 4) is plotted versus the energy of the incoming field. No damping terms in eq 1 are introduced at the resonances. Vertical lines show the two-photon resonances associated with the Q and the Soret band transitions of DZnDPPA. INDO/SCI calculations are known to have an error of $\pm 2000$ cm$^{-1}$ for the transition energies. From this viewpoint, arrow 1 marks the theoretically calculated $\beta_{vec}$ (1.06 $\mu$m) and arrow 2 shows the estimated value of $\beta_{vec}$ ("1.06 $\mu$m") arrived at by shifting the incident photon energy to be 0.18 eV away from the two-photon resonance related to the Soret transition (see text and Figure 4 caption).

**Table 3.** Calculated Values of $\beta$ at 1.06 $\mu$m for Molecules **II**−**VIII**[a]

| molecule | INDO-SOS (calcd) | exptl (EFISH)[10] | exptl (HRS)[15] |
|---|---|---|---|
| **II** | 106.7 | | |
| **III** | 147.5 | | |
| **IV** | 477.3 | | 4933 |
| **V** | 50.9 | | |
| **VI** | 95.3 | $30 \pm 10$ | |
| **VII** | 53.6 | $20 \pm 10$ | |
| **VIII** | 65.2 | $\leq 10$ | |

[a] The experimental values of molecules **IV**, **VI**, **VII**, and **VIII** are taken from refs 10 and 15. All values aer in units of $10^{-30}$ cm$^5$/esu.

contribution from ($\Delta\mu_{ng}\mu^2_{ng}\Delta E_{gn}{}^{-2}$), as the energy denominator becomes large for the higher excited states.

In Figure 8, the frequency-dependent $\beta$ values are presented for chromophores **II**−**IV**. In calculating $\beta$, no damping terms were included in the $\beta$ expression, despite the fact that $\beta$ has resonances at $\Delta E_{gn}$ and $\Delta E_{gn}/2$. The frequency dependence of $\beta$ values for D−ZnDPP−A parallel the values for ZnDPP−A away from the resonance. The sum of $\beta$ values for D−ZnDPP and for ZnDPP−A is less than but of the same order of magnitude as that calculated for D−ZnDPP−A. A simple additivity rule like this does not hold for simpler molecules like *p*-nitroaniline. The computed values of $\beta$ at 0.830 and 1.064 $\mu$m are $8162 \times 10^{-30}$ and $471 \times 10^{-30}$ cm$^5$/esu, respectively. Using the offset frequencies discussed above (introduced so that the input frequency appears at the experimental[12] offset from the Soret transition), we compute $\beta$ values of $4996 \times 10^{-30}$ and $1184 \times 10^{-30}$ cm$^5$/esu, respectively. The experimental measurements of $\beta$ at 0.830 and 1.064 $\mu$m are the same ($\sim$5000 $\times 10^{-30}$ cm$^5$/esu), within experimental error. The corrected computed values differ from each other by about a factor of 4. Further investigation of the frequency dependence of $\beta$ on both experimental and theoretical levels is in order.

The calculated $\beta$ values at 1.064 $\mu$m for molecules **II**−**VIII** are given in Table 3, as are the experimental values.[10] Note that, relative to molecules **II**−**IV**, the calculated values of $\beta$ vary little throughout the series defined by compounds **V**−**VIII** as a function of aryl group composition. As was recognized earlier,[10] this effect derives mainly from the fact that the large dihedral angle between the aryl groups and porphyrin core severely restricts the magnitude of the conjugative interactions between the aromatic ring systems in compounds **V**−**VIII**. This reduced coupling dampens all three terms $\Delta\mu_{ng}$, $\mu^2_{ng}$, and $\Delta E_{gn}{}^{-2}$. This is clearly not the case for molecules **II**−**IV**. Our calculations underscore the important role that arylethynyl moieties can play in the modulation of chromophore electronic properties via conjugative interactions. These arylethynyl groups can also serve to tune the magnitudes of the key parameters that control $\beta$ in porphyrin-based NLO chromophore systems.

**Table 4.** Calculated Values of $\beta$ using Eqs 6 and 1[a]

This Work

| molecule | $\beta_{zzz}$ (eq 1) | $\beta_{ZZZ}$ (eq 6) |
|---|---|---|
| D−Zn−DPP−A | 479.4 | 481.2 |
| D−ZnDPP−A (partial cumulenic character) | 1890.1 | 1888.1 |

Results of Ref 22

| | INDO-SOS (calcd) | HRS (exptl) |
|---|---|---|
| $\beta$-cyclocitral | 3.8 | 5.0 |
| $\beta$-ionone | 15.8 | 10.0 |
| retinal | 108.0 | 270.0 |
| carotenal | 538.5 | 1040.0 |

[a] Also presented are the experimental (HRS) values and calculated INDO values from ref 22. All values are in units of $10^{-30}$ cm$^5$/esu at 1.06 $\mu$m.

Spectroscopic studies have shown that ehynyl or butadiynyl bridging groups that directly link the carbon frameworks of a porphyrin to the macrocyclic periphery of additional porphyrins or other aromatic entities can define superstructures with substantial excited-state charge delocalization.[12,14,15] In an attempt to study the effect of this electronic delocalization, we have calculated the hyperpolarizability of a model cumulenic structure of D−ZnDPP−A, where the bond lengths of the three C−C bonds of the conjugated bridge linking D to ZnDPP and A to ZnDPP are made equal to each other (without changing the structure within the porphyrin ring).[32] Table 4 summarizes the results of these calculations. The calculated value of $\beta$ at 1.064 $\mu$m is $1845 \times 10^{-30}$ cm$^5$/esu for the cumulenic D−ZnDPP−A, while for a gas phase optimized geometry, it is $479 \times 10^{-30}$ cm$^5$/esu, underscoring the importance of bond length alternation in controlling the optical nonlinearities.[33] In general, such enhancements in $\beta$ are derived from a decrease in the HOMO/LUMO gap energy and an increase in $\mu_{ge}$.

The calculated values of $\beta_{ZZZ}$ (1.06 $\mu$m) in the laboratory frame of reference using eq 6 are compared with the corresponding molecular tensor elements in Table 4. In D−ZnDPP−A, the molecular tensor element in the direction of the charge transfer axis is the largest, the values of $\beta_{ZZZ}$ are within 2% of $\beta_{zzz}$. Table 4 also shows recently reported[22] $\beta$ values for a variety of organic chromophores, obtained by HRS experiments and INDO/S calculations. A similar trend for experimental and theoretical $\beta$ values is obtained in our work.

(32) The selected bridge bond lengths are as follows: (A) in the gas phase $R$(C1−C2) = 1.4 Å, $R$(C2−C3) = 1.2 Å, and $R$(C3−C4) = 1.4 Å; (B) in the cumulenic structure all the above bond lengths are made equal to 1.33 Å. Here C1 corresponds to the 1′-C of the aryl group, C2 is the acetylenyl group carbon linked to the 1′-C atom, and C3 is other ethynyl group carbon bonded to the *meso* carbon (C4) of the porphyrin.

(33) (a) Marder, S. R.; Beratan, D. N.; Cheng, L.-T. *Science (Washington, DC)* **1991**, *252*, 103−106. (b) Risser, S. M.; Beratan, D. N.; Marder, S. R. *J. Am. Chem. Soc.* **1993**, *115*, 7719−7728. (c) Bourhill, G.; Bredas, J.-L.; Cheng, L.-T.; Marder, S. R.; Meyers, F.; Perry, J. W.; Tiemann, B. G. *J. Am. Chem. Soc.* **1994**, *116*, 2619−2620. (d) Marder, S. R.; Gorman, C. B.; Meyers, F.; Perry, J. W.; Bourhill, G.; Bredas, J.-L.; Pierce, B. M. *Science (Washington, DC)* **1994**, *265*, 632−635.

(34) Yu, J.; Zerner, M. C. *J. Chem. Phys.* **1994**, *100*, 7487−7494.

The computed values of $\langle\beta_{ZZZ}^2\rangle^{1/2}$ at 1.064 and at 0.830 $\mu$m (using the frequency offsets discussed above) are within a factor of 2−3 of the experimental values and are within a factor of 4 of each other. This factor of 2 can be understood upon the basis of the analysis by Yu and Zerner,[37] which shows that the calculated gas-phase $\beta$ values are approximately doubled in the presence of solvent. Without using the frequency offsets, the values are underestimated by about 1 order of magnitude. The $\beta$ values computed are a function of the transition energies, which are challenging to compute with certainty in the large molecules under investigation here.

## 4. Conclusions

The theoretical absorption spectrum calculated for D−ZnDPP−A is in qualitative agreement with the experimental spectrum. The Q and Soret transitions of D−ZnDPP−A are both red shifted with significantly increased extinction coefficients and highly broadened absorption bands relative to the parent ZnDPP molecule. The excited states of D−ZnDPP−A cannot be explained satisfactorily in the context of a four-orbital model, due to the strong mixing of high-energy singly excited configurations involving the D and A units. Detailed analysis of the electronic properties of these and other conjugated porphyrin systems will be presented separately.[29]

Charge transfer and two-state analyses were used successfully to explain the origin of the first electronic hyperpolarizability in D−porphyrin−A molecules that feature two distinct arylethynyl moieties. A simple calculation of the charge change on the bridge (in this case ZnDPP) associated with a specific excited state is sufficient to predict how that term influences the EBS sum. States with an increase in electron density on the bridge lead to a decrease in $|\beta|$ in most cases; the extent of the increase or decrease of the $\beta$ value associated with a given basis state is proportional to the size of the two-state-like product (eq 2).

Previously studied D−porphyrin−A systems (**VI**−**VIII**) in which the electron-donating and -withdrawing entities are amino- and nitro-substituted *meso*-aryl groups, respectively, do not exhibit large $\beta$ values since there is not substantial electronic communication between d and a.[10] Electronic communication has been limited by the torsional barrier to rotation about the porphyrin-to-*meso*-phenyl bond, resulting in all the excited-state configurations being essentially porphyrin-localized. As a result of this, the calculated $\beta$ values for these other species vary little with aryl group composition, although theory correctly predicts that molecule **VI**, with two 4′-aminophenyl donors and two 4″-nitrophenyl acceptors in a *syn* conformation, should have the largest $\beta$ value within this series. Theory further predicts that the acetylenyl-bridged D−porphyrin−A molecule (D−ZnDPP−A) to have an extremely large first hyperpolarizability, consistent with the recently reported experimental results.[12] This value is expected to depend, in part, upon a small predicated contribution of the cumulenic resonance structure to the ground state.

In poled polymer devices the experimentally relevant quantity is often $\mu\beta$. The converged value of $\mu\beta$ after a sum over 50 EBS is $1806 \times 10^{-48}$ cm$^5$/esu (zero frequency) and $2548 \times 10^{-48}$ cm$^5$/esu (1.907 $\mu$m). The $\mu\beta$ values calculated using the two-state model,[35,36] where only the first charge transfer excited state is included, are $4957 \times 10^{-48}$ (zero frequency) and $6659 \times 10^{-48}$ cm$^5$/esu (1.907 $\mu$m); the two-state model[35,36] thus overestimates the converged value by about a factor of 4.

These calculations suggest that it should be possible to build acetylenyl-bridged D−porphyrin−A complexes with extremely large molecular first hyperpolarizabilities, surpassing even that observed for the D−ZnDPP−A complex. For example, one of the largest experimentally determined $\mu\beta$ values reported for a small molecule is $8600 \times 10^{-48}$ cm$^5$/esu measured at 1.907 $\mu$m in chloroform for a diarylthiobarbituric acid derivative.[37] In an attempt to demonstrate the utility of longer conjugated chromophore bridges based upon the ethynyl-substituted porphyrin structural motif, $\beta$ was calculated for {[5,-((4″-(dimethylamino)phenyl)ethynyl)-10,20-diphenylporphinato]zinc(II)}−{[5′-((4‴-nitrophenyl)ethynyl)-10′,20′-diphenylporphinato]zinc(II)}ethyne (D−ZnDPP−ZnDPP−A, **IX**), in which two ZnDPP units are wired together by an ethynyl bridge connecting the chromophores at their respective 5- and 5′-positions; (4″-(dimethylamino)phenyl)ethynyl and (4‴-nitrophenyl)ethynyl groups are located at opposite ends of the supramolecular chromophore at the 15- and 15′-positions, respectively (Figure 9). The calculated $\beta$ value for D−ZnDPP−ZnDPP−A is nearly twice as large as that calculated for D−ZnDPP−A, while the associated $\mu\beta$ values (both at 1.907 $\mu$m) obtained for the two compounds were $3299 \times 10^{-48}$ and $2548 \times 10^{-48}$ cm$^5$/esu, respectively. This calculation is consistent with the proposal that high oscillator strength, bridge-centered transitions oriented along the D-to-A vector provide a viable strategy to simultaneously enhance $\Delta\mu_{ng}$, $\mu^2_{ng}$, and $\Delta E_{gn}{}^{-2}$.[1,12]

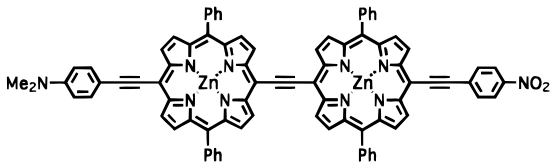


$\beta = 742.1 \times 10^{-30}$ cm$^5$/esu (at 1.06 μm)

**Figure 9.** Structure of {[5,-10-((4″-(dimethylamino)phenyl)ethynyl)-10,20-diphenylporphinato]zinc(II)}−{[5′,-10′-((4‴-nitrophenyl)ethynyl)-10′,20′-diphenylporphinato]zinc(II)}ethyne (D−ZnDPP−ZnDPP−A, **IX**) and its calculated $\beta_{vec}$ value at 1.06 $\mu$m incident irradiation. The calculation is based upon a structure with bond lengths analogous to those of the ground-state D−ZnDPP−A structure.

Versatile, well-established synthetic methodology permits the design and synthesis of a variety of highly conjugated D-bridge-A complexes in which the chromophoric, largely bridge-centered excited states enable strong D−A electronic coupling.[12−15,38] The extraordinary photophysics of such compounds define a new design direction for organic nonlinear optical compounds.[12,14] Future theoretical and experimental work shall elucidate how the D, A, and conjugated bridge structure, bridge length, bridge polarizability, chromophore photophysics, and porphyrin metals effect the molecular first-order hyperpolarizability in such D−bridge−A species.

**Acknowledgment.** D.N.B. thanks the National Science Foundation (Grant Nos. CHE-9257093 and CHE-9106689) for partial support of this work. M.J.T. acknowledges the Office of Naval Research (O.N.R. N000149510725) for support. We thank Dr. R. Bendale and Professor M. C. Zerner for providing the ZINDO program and Dr. M. Thompson for the ARGUS package. We are grateful to Dr. S. M. Risser and Mr. Steven M. LeCours for helpful discussions.

JA952690Q

(35) Oudar, J. L. *J. Chem. Phys.* **1977**, *67*, 446−457.
(36) Oudar, J. L.; Chemla, D. S. *J. Chem. Phys.* **1977**, *66*, 2664−2668.
(37) Gilmour, S.; Montgomery, R. A.; Marder, S. A.; Cheng, L.-T.; Jen, A. K.-Y.; Cai, Y.; Perry, J. W.; Dalton, L. R. *Chem. Mater.* **1994**, *6*, 1603−1604.
(38) (a) DiMagno, S. G.; Lin, V. S.-Y.; Therien, M. J. *J. Am. Chem. Soc.* **1993**, *115*, 2513−2515. (b) DiMagno, S. G.; Lin, V. S.-Y.; Therien, M. J. *J. Org. Chem.* **1993**, *58*, 5983−5993.